

Influence of Ni dopant on the Structural and Electrical Properties of ZnFe_2O_4 nanoparticles

*Uzma G, Qaiser H, Asma S,

Abstract. Nano-crystalline $\text{Ni}_x\text{Zn}_{1-x}\text{Fe}_2\text{O}_4$ ($x = 0, 0.1, 0.3, 0.5, 0.7$) were synthesized using chemical co-precipitate method and sintered at 700°C to study the effect of Nickel doping on the properties of ZnFe_2O_4 nanostructures. Debye-Scherrer formula is used to calculate the average crystalline size, shows a decreasing value at lower concentrations of Ni, and increases further due to the mixed spinel structure of prepared ferrites. Decreasing trend in lattice parameters and d-spacing with increase in Ni^{2+} contents can be explained on the basis of ionic radius and lattice stress-strain produced by Ni ions. A decreasing trend in the dielectric constant (ϵ') and dielectric loss tangent ($\tan\delta$) with increasing frequency and Ni concentration is in accordance with the Maxwell-Wagner type interfacial polarization. Moreover, an increasing trend of ac conductivity (σ_{ac}) with increasing frequency and decreasing with nickel concentration is also reported due to the reduction of Fe^{+3} ions in octahedral sites as a result of larger coulomb field in its locality.

Keywords: Chemical Synthesis; Co-precipitation method, Nano particles, X-ray diffraction; dielectric properties; electrical conductivity

1 INTRODUCTION

Many researchers have worked on Nano-crystalline Ni-Zn spinel ferrites in the last few decades due to its enormous commercial and defense (at high frequency) applications. Ni-Zn ferrites have mixed spinel structure as in nickel ferrites (NiFe_2O_4) the crystal field stabilization energy (CFSE) of Ni^{+2} at octahedral field is greater than that of Fe^{+3} shows the inverse spinel structure whereas in zinc ferrite (ZnFe_2O_4) the CFSE of Zn^{+2} at octahedral field is equal to that of Fe^{+3} shows a normal spinel structure [1, 2].

As the selection of synthesis process have great influence on the performance of ferrites for all types of application therefore, in the present research chemical co-precipitation method has been chosen due to its easy handling, low temperature, narrow size distribution, obtained well disperse particles and low cost [3] to synthesize mixed Ni-Zn spinel ferrites by the addition of Ni^{+2} ions which alters the distribution of ions in the spinel ferrite structure and have very low tangent losses even for high frequency applications such as for transformer core and especially for application in defense as radar absorbing materials [4].

2 MATERIALS & METHODS

Series of Ni-Zn ferrites were prepared with composition of $\text{Ni}_x\text{Zn}_{1-x}\text{Fe}_2\text{O}_4$ ($x = 0, 0.1, 0.3, 0.5, 0.7$) by co-precipitation method. The materials being used were processed on a hot magnetic plate at 80°C to achieve a pH level of 11~12. The liquid precipitate was then stirred for one hour and was brought to room temperature. The prepared precipitate was first washed twice and dried at 100°C overnight.

After completely drying, converted to fine powder by grinding. Finally, the prepared samples were annealed at a temperature of 700°C for five hours to get the nanoparticles.

For dielectric study, pellets were obtained by pressing the powder at a pressure of 2ton/inch². For better electrical contacts, the pellets were coated with silver paint. Powder X-ray diffraction (XRD) measurements were carried out to identify the phase. The dielectric properties including dielectric constant, tangent loss and ac conductivity were studied for all samples in the frequency range of 1 kHz to 2 MHz by Inductance Capacitance resistance method (LCR) 7600 plus precision meter.

3 RESULTS AND DISCUSSION

3.1 Structural Study

X-ray diffraction (XRD) measurements were carried out to determine the phase purity and crystallographic structure of the samples with Cu K α radiation having wavelength $\lambda=1.5405\text{\AA}$. The XRD data were collected by step scanning over an angular range of $20^\circ \leq 2\theta \leq 80^\circ$ at a step size of 0.025° and counting time of 0.4 seconds per step. The X-Ray diffraction patterns for $\text{Ni}_x\text{Zn}_{1-x}\text{Fe}_2\text{O}_4$ ($x= 0, 0.1, 0.3, 0.5, 0.7$) nano-crystals sintered at 700°C have been shown in Fig.1, confirms the formation of cubic spinel structure. Peak position, average crystalline size, d-spacing, and lattice parameter values have been calculated and listed in table 1 corresponding to (311) plane. From data a slight shift of XRD peaks of 2θ from 35.0308 to 35.3151 was observed corresponding to (311) plane, which confirms the replacement of Zn^{2+} ions by Ni^{2+} ions.

3.1.1 Size variation with Composition

For the calculation of average crystallite size D Scherer formula is used [2, 5]

$$D = 0.9\lambda/\beta \text{ Cos}\theta \quad (1)$$

" D " is the crystal size, " λ " is X-ray wavelength, " β " represents full width at half maxima (FWHM) and θ is the Bragg's diffraction angle at the 2θ scale. From table (1) it can be seen that at $x=0$, the crystal size becomes 58nm, but with the doping of Ni contents the particle size varies between 18nm to 36nm. Crystalline size first decreases and then increases due to the mixed spinel structure of prepared ferrites.

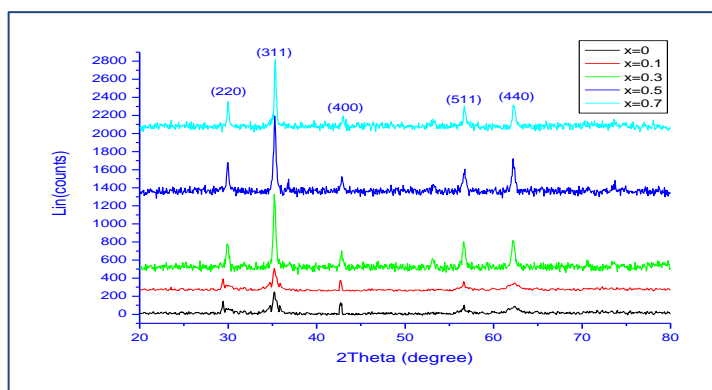


Fig. 1: X-ray diffraction pattern of $\text{Ni}_x\text{Zn}_{1-x}\text{Fe}_2\text{O}_4$

3.1.2 Lattice parameter variation with composition

Lattice parameter values calculated and listed in table (1) using following equation for different nickel contents.

$$a = d\sqrt{h^2 + k^2 + l^2} \quad (2)$$

“d” is inter-planar distance, (h k l) are Miller indices. Table (1) and figure (2) describe that the lattice parameter decreases for smaller Zn²⁺ contents and vice versa. The decrease in lattice parameter with increase in Ni²⁺ contents can be explained as the ionic radius of Ni²⁺ (0.7Å) is smaller than the ionic radius of Zn²⁺ (0.82Å) as reported by other authors [6-8].

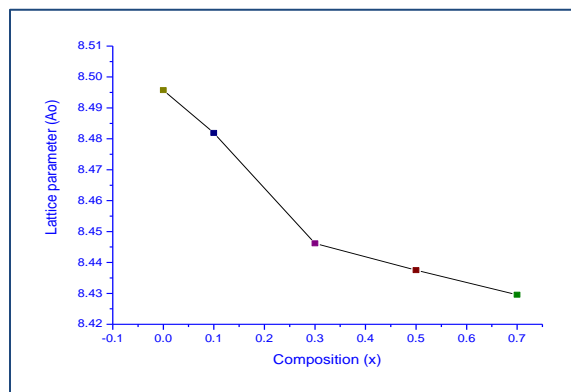


Fig 2: Variation of lattice parameter in Ni_xZn_{1-x}Fe₂O₄ with Composition (x)

x	Peak position (2θ°)	Crystal size (nm)	d _(h,k,l) spacing (Å°)	Lattice parameter (Å°)	Lattice strain
0	35.0308	58	2.56157	8.49576	0.0020
0.1	35.0900	18	2.55739	8.48190	0.0068
0.3	35.2433	29	2.54662	8.44618	0.0041
0.5	35.2807	36	2.54400	8.43749	0.0032
0.7	35.3151	36	2.54161	8.42957	0.0032

3.1.3 d-spacing variation with composition

The values of “d” have been calculated by Bragg’s equation and listed in table (1).

$$2d \sin \theta = n\lambda \quad (3)$$

From table (1), the values of d-spacing between lattices planes decrease with the increase of Ni concentration. This can be described by the concept that Ni ions produce lattice stress and strain which cause a reduction in d-spacing in the material as shown in Figure (3).

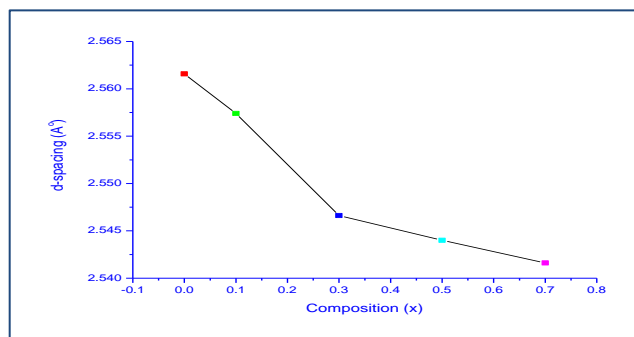


Fig.3: Variation of d-spacing in Ni_xZn_{1-x}Fe₂O₄ with composition (x)

3.2 Dielectric Study

The real part (ε') and imaginary part (ε'') of dielectric constant, tangent loss (tanδ) and AC conductivity (σ_{ac}) were studied for all samples with the test frequency (f) in the range of 1kHz to 2MHz by using LCR 7600 plus precision meter and determined using the following equations. Where, “C” is the capacitance of our sample, “d” is for spacing between the plates, and “A” represents the area of the sample between the plates of the capacitor and ε₀ is the permittivity of free space, and ω is the angular frequency.

3.2.1 Variation in dielectric constant(ϵ') with frequency and Ni concentration

Response of dielectric constant with frequency shows behavior like typical ferrimagnetic materials, i.e. at low frequency dielectric constant has a larger value and decreases with the increase in frequency as shown in Fig 4(a). At low frequency, higher values of dielectric constant may be explained on the basis of Maxwell-Wagner model telling that ferrites comprise of very conducting grains alienated by weakly conducting grain boundaries [9]. Due to this behavior, electrons may pile up at grain boundaries since hopping leading to polarization but this hopping frequencies cannot follow the AC field variation at higher frequencies and results in constant performance of permittivity.

The conduction process in ferrite materials is caused by electrons jumping between Fe^{+2} and Fe^{+3} ions. When the frequency of the field increases beyond 1 kHz, the field frequency cannot be followed by hopping electrons and begin decreasing. The grain size for $x = 0.1$ is smaller as compared to other samples, therefore, even at relatively greater values of frequency results in increasing the hopping electron probability which makes the value of the dielectric constant greater relative to other samples. This is because of the high resistivity value and relatively smaller size of the crystallite of this sample. For $x = 0.3, 0.5$ and 0.7 samples, the grain size again goes to increase but due to the increase of Ni^{+2} concentration, lesser quantity of Fe^{+3} ions decreases the probability of hopping and hence the dielectric constant decreases. The dielectric constant decreasing trend as a function of frequency may be due to the fact that exchange of electrons between cations cannot follow the frequency pattern obeying the Debye relaxation process [10]. Figure (4b) explains the dielectric constant variation with different Ni concentrations at 100, 1000, and 2000 kHz. By increasing the nickel concentration, the dielectric constant is going to decrease. [5, 11]. Further, at octahedral [B] sites where the cations have strong preference, lead to replace Fe^{+3} ions. Furthermore, the decreasing trend in dielectric constant is due to the fact that in the conduction process [12], Ni^{+2} ions do not take part results in a decrease in electron hopping.

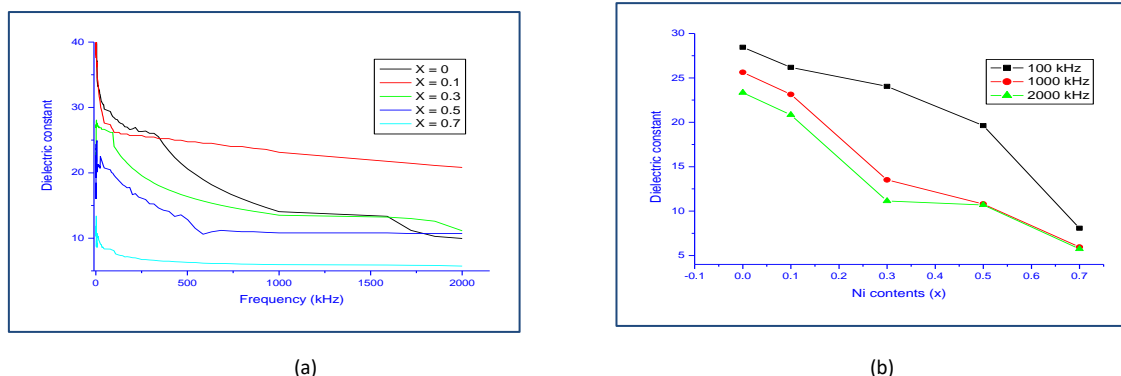
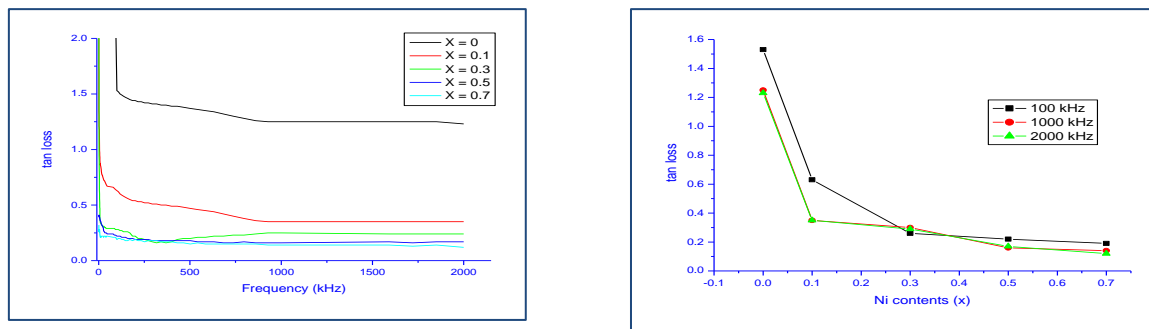


Fig.4 (a, b): Variation in dielectric constant (ϵ') in $\text{Ni}_x\text{Zn}_{1-x}\text{Fe}_2\text{O}_4$ with frequency and Ni concentration (x)

3.2.2 Variation of tangent loss ($\tan\delta$) with frequency and Ni concentration (x)

The dielectric tangent loss ($\tan\delta$) is related to energy loss by dipole rotation and domain wall motion by alternating electric field. Figure (5) describes the tangent loss variation with frequency, same trend as in case of dielectric constant. The loss is very high at low frequencies, which may be due to a large quantity of heat dissipation during domain wall motions. But this motion inhibits with increasing frequency and due to rotation, polarization may be forced to alter their position, and this rotation does not respond at higher frequency; hence a lesser quantity of heat is dissipated. From

Figure (4a) and Figure (5) it is clear that with increasing frequency both the dielectric constant and tangent loss initially decrease and then become saturated. For an explanation of this phenomenon, we may take the help of Koops' model [10, 12]. Variation of tangent loss ($\tan\delta$) with Ni concentration (x) decreases, which indicates that for higher values of tangent loss, the larger grain are responsible. Figure (5b) shows the tangent loss variation with different Ni concentration at 100, 1000 and 2000 kHz.



(a)

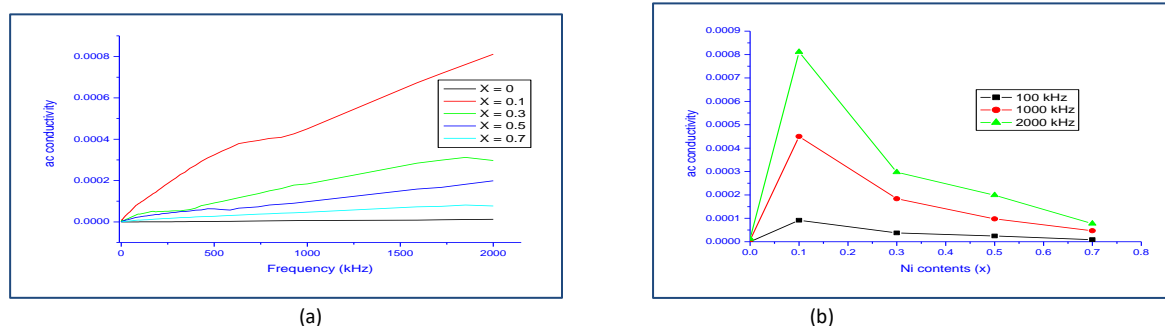
(b)

Fig. 5(a, b): Variation of tan loss in $\text{Ni}_x\text{Zn}_{1-x}\text{Fe}_2\text{O}_4$ with frequency and Ni concentration (x)

3.2.3 Variation of ac conductivity (σ_{ac}) with frequency and Ni concentration (x)

Figure (6a) illustrates the ac conductivity variation with frequency. AC conductivity increases with increasing frequency and follows the law of dynamic [13] $\sigma(\omega) = A\omega^s$, in which "s" stands for linear plot slope of frequency-dependent conductivity and A is a parameter having unit of conductivity.

The "s" values lie between 0 and 1 and may never exceed these limits [14]. Maxwell–Wagner model [9] may best explain frequency-dependent conduction processes. With increase in concentration of Ni^{2+} from $x = 0.1$ to $x = 0.7$ which produces larger coulomb field in its locality and hence Fe^{+3} ions reduces in octahedral sites, which results in smaller value of conductivity. The increase in conductivity in sample at $x=0.1$ is due to smaller grain size as clear from table 1 and may also due to cations redistribution on octahedral (B) and tetrahedral (A) sites which form a mixed cationic distribution Figure (6b) indicates the ac conductivity variation with different Ni concentration at 100, 1000 and 2000 kHz. The samples conductivity shows an augmentation from $x = 0$ to $x = 0.1$ due to smaller grain size and then decreases with further increase in Ni^{2+} concentrations. The smaller amount of Fe^{+3} ions are responsible for reducing the probability of the ion exchange between Fe^{+3} and Fe^{+2} , which results in decreasing conductivity.



(a)

(b)

Fig.6 (a, b): Variation of AC conductivity in $\text{Ni}_x\text{Zn}_{1-x}\text{Fe}_2\text{O}_4$ with frequency and Ni Concentration (x)

4 CONCLUSION

Chemical co-precipitation method was used for synthesis of nano-crystalline Ni-Zn ferrites having chemical formula $Ni_xZn_{1-x}Fe_2O_4$ ($x=0, 0.1, 0.3, 0.5, 0.7$) in this research. For obtaining a good crystalline phase, the prepared powder was sintered for five hours at 700°C. The formation of a single phase cubic spinel structure was confirmed from powder x-ray diffraction results. Average crystallite size was calculated by using the Scherrer formula and found to be in the range of 18-36nm with the doping of Ni contents and 58nm at $x = 0$. The lattice parameter values were found to decrease with increase in Ni concentration from 8.495Å to 8.429Å due to smaller radius of nickel and d-spacing were also found to decrease from 2.561 Å to 2.541 Å due to the reason that Ni ions produce lattice stress and strain which make reduction in d-spacing.

A decreasing trend in the dielectric constant (ϵ') and dielectric loss tangent ($\tan\delta$) w.r.t increasing frequency and Ni concentration is reported and described by Maxwell-Wagner model and Koop's model respectively. Moreover, the increasing trend of ac conductivity (σ_{ac}) w.r.t increasing frequency and nickel concentration is also described using Maxwell-Wagner model and dynamic law.

ACKNOWLEDGMENTS

This work is supported by Department of Physics, University of Wah, Wah Cantt Pakistan.

5 REFERENCES

- [1] M. Ajmal, A. Maqsood, "Influence of zinc substitution on structural and electrical properties of $Ni_{1-x}Zn_xFe_2O_4$ ferrites," *Mater. Sci Eng.: B*, vol. 139, no.2-3, pp. 164-170, 2007. <https://doi.org/10.1016/j.mseb.2007.02.004>.
- [2] S. Li, J. Pan, F. Gao, *et al.*, "Structure and magnetic properties of coprecipitated nickel-zinc ferrite-doped rare earth elements of Sc, Dy, and Gd," *J Mater Sci: Mater Electron*, vol. 32, pp. 13511-13526, 2021. DOI: [10.1007/s11801-021-05967-y](https://doi.org/10.1007/s11801-021-05967-y).
- [3] R. Sen and P. Jain, "Synthesis and Characterization of Nickel Ferrite ($NiFe_2O_4$) Nanoparticles Prepared by Sol- Gel Method," *Materials Today: Proceedings*, vol. 2, no. 4-5, pp. 3750-3757, 2015.
- [4] S. Slimani, C. Meneghini, M. Abdolrahimi, *et al.*, "Spinel Iron Oxide by the Co-Precipitation Method: Effect of the Reaction Atmosphere," *Appl. Sci.* vol. 11, pp. 5433, 2021. <https://doi.org/10.3390/app11125433>
- [5] J. Madhavi, "Comparison of average crystallite size by X-ray peak broadening and Williamson-Hall and size-strain plots for VO^{2+} doped ZnS/CdS composite nanopowder," *SN Appl. Sci.* vol. 1, pp. 1509, 2019. <https://doi.org/10.1007/s42452-019-1291-9>
- [6] G. S. Shahane, A. Kumar, M. Arora, *et al.*, "Synthesis and characterization of Ni-Zn ferrite nanoparticles", *J. Magn. Mater.* vol. 322, no. 8, pp. 1015-1019, 2010. <https://doi.org/10.1016/j.jmmm.2009.12.006>.
- [7] Uzma G, Study of electrical properties of Cu-Zn ferrite with Si additive, *Kovove Materialy Metalic Mater.* Vol. 50, no. 39-42, 2012. [doi:10.4149/km.2012.1.39](https://doi.org/10.4149/km.2012.1.39)
- [8] P. Punia, R. Dhar, B. Ravelo, *et al.*, "Microstructural, Optical and Magnetic Study of Ni-Zn Nanoferrites", *J Supercond Nov Magn*, vol. 34, pp. 2131-2140, 2021. <https://doi.org/10.1007/s10948-021-05967-y>
- [9] A. Radoń, D. Łukowiec, M. Kremzer, *et al.*, "Electrical Conduction Mechanism and Dielectric Properties of Spherical Shaped Fe_3O_4 Nanoparticles Synthesized by Co-Precipitation Method", *Materials*, vol. 11, no. 735, 2018. <https://doi.org/10.3390/ma11050735>
- [10] A. Verma, T.C. Goel, R.G. Mendiratta, *et al.*, "Dielectric properties of NiZn ferrites prepared by the citrate precursor method", *Mater Sci and Engin: B*, vol. 60, no. 2, pp. 156-162, 1999.
- [11] Uzma G, "Effect of Si on the dielectric properties of $Ni_xZn_{1-x}Fe_2O_4$ as a function of composition and frequency," *IJPAP*, vol. 53, no. 4, pp. 271-273, 2015.

- [12] C. G. Koops, " On the Dispersion of Resistivity and Dielectric Constant of Some Semiconductors at Audio frequencies", *Phys. Rev.* vol. 83, no. 1, pp. 121-124, 1951.
- [13] S.S Khemalpure, P.L Hosamani, S.N Mathad, *et al*, "Synthesis, structural and dielectric properties of Ni-Zn-Cu ferrites", *Advan Science, Engin and Medicine*, vol.1, no.11(5), pp. 375-82, 2019.
<https://doi.org/10.1166/asem.2019.2363>
- [14] W. R Agami, "Effect of neodymium substitution on the electric and dielectric properties of Mn-Ni-Zn ferrite", *Physica B: Condensed Matter*, vol.1, no.534, pp.17-21, 2018. <https://doi.org/10.1016/j.physb.2018.01.021>

Corresponding Author, Prof Uzma Ghazanfar is currently serving as Professor in Department of Physics, Universit of Wah, Wah Cantt Pakistan,

PH-092-51-9157722. E-mail: uzma.ghazanfar@uow.edu.pk